J Therm Anal Calorim (2016) 123:2053–2060
DOI 10.1007/s10973-015-4711-0

Thermal studies of analgesic active 8-aryl-2,6,7,8-tetrahydroimidazo[2,1-*c*][1,2,4]triazine-3,4-diones

Agata Bartyzel[1] · Małgorzata Sztanke[2] · Krzysztof Sztanke[2,3]

Received: 5 January 2015 / Accepted: 14 April 2015 / Published online: 1 May 2015

Abstract This article describes the determination of thermal stability by investigating the thermal degradation of six analgesic active derivatives of 8-aryl-2,6,7,8-tetrahydroimidazo[2,1-*c*][1,2,4]triazine-3,4-dione (8-ATHITD). The compounds under study were characterized by TG–DSC and TG–FTIR analyses. The investigated compounds are stable at room temperature which is important for medical application. Thermogravimetric measurements in air atmosphere showed that the decomposition of compounds proceeds in the two main stages. The first mass loss steps are observed in the temperature ranges of 261–305 °C and occurred together with the melting process for the majority of studied compounds. It was also noted that the *para* isomers are found to be more thermal stable than their *ortho* analogues as a consequence of a higher symmetry of compounds. Based on the obtained data from the TG–FTIR analysis, the main gaseous products resulting at thermal degradation are CO_2, CO, NH_3, HCN, HNCO (and its derivatives), aniline or its derivatives and carbonyl compounds.

Keywords Analgesic agents · Fused 1,2,4-triazinediones · Thermal studies · TG–DSC · TG–FTIR

✉ Agata Bartyzel
agata.bartyzel@poczta.umcs.lublin.pl

[1] Department of General and Coordination Chemistry, Maria Curie-Skłodowska University, Maria Curie-Skłodowska Sq. 2, 20-031 Lublin, Poland

[2] Chair and Department of Medical Chemistry, Medical University, 4A Chodźki Street, 20-093 Lublin, Poland

[3] Laboratory of Bioorganic Synthesis and Analysis, Chair and Department of Medical Chemistry, Medical University, 4A Chodźki Street, 20-093 Lublin, Poland

Introduction

The undesirable changes in the crystalline structure, composition and physicochemical properties of the candidate drug for pharmaceutical use may evoke the decrease in its activity or even increased toxicity. Therefore, the combined and coupled thermal analysis techniques proved to be applicable as very reliable in studies of the stability, decomposition and purity of biologically active lead structures [1–5].

In the present paper, we would like to give an impression about the thermal behaviour of six tetrahydroimidazotriazinediones (**1–6**), considered for further more detailed drug-development studies. Therefore, it seems worthwhile to estimate the enthalpy of fusion of these compounds and the range of their thermal stability and to identify the gaseous products of thermal decomposition of these compounds. The combined and coupled thermal techniques such as TG–DSC, TG–DTA and TG–FTIR were recommended for a description of thermal stability and an identification of the products of their thermal decomposition. Thermal analyses of the compounds under study were carried out by the TG–DSC (air) and TG–FTIR (nitrogen) techniques. We have chosen TG–DSC analysis because these techniques provide information on the content volatile components such as solvents or water, on decomposition behaviour and on the ash content as well as on the thermal effects which are characterized by an enthalpy change and by the temperature range, such as melting behaviour, crystallization, solid–solid transitions and chemical reactions [2, 3, 5]. These techniques have been used by us to determine the temperature and heat of fusion as well as the range of thermal stability of each compound. The TG–FTIR measurements provided additional information about residual solvents and volatile

pyrolysis products [5–7]. These results are very important factors since the determination of the temperature range in which a certain medicine substance is stable regarding its structure as well as its pharmaceutical action is crucial for stocking drugs, for its technological transformations and for the obtaining technology of the right formulas.

The following compounds from the title class were used in thermal studies: 8-phenyl-2,6,7,8-tetrahydroimidazo[2,1-*c*][1,2,4]triazine-3,4-dione (**1**), 8-(2-methylphenyl)-2,6,7,8-tetrahydroimidazo[2,1-*c*][1,2,4]triazine-3,4-dione (**2**), 8-(4-methylphenyl)-2,6,7,8-tetrahydroimidazo[2,1-*c*][1,2,4]-triazine-3,4-dione (**3**), 8-(2-methoxyphenyl)-2,6,7,8-tetrahydroimidazo[2,1-*c*][1,2,4]triazine-3,4-dione (**4**), 8-(4-methoxyphenyl)-2,6,7,8-tetrahydroimidazo[2,1-*c*][1,2,4]triazine-3,4-dione (**5**), 8-(3-chlorophenyl)-2,6,7,8-tetrahydroimidazo[2,1-*c*][1,2,4]triazine-3,4-dione (**6**). Chemical structures that distinguish these derivatives are shown in Scheme 1.

The compounds investigated (**1**, **3–6**) have previously been identified as capable of revealing first and foremost analgesic effects in vivo combined with relatively low acute toxicities [8, 9]. The most promising small molecules, such as: **6** (LD_{50} in mice if injected intraperitoneally: over 2000 mg kg^{-1}) and **5** (LD_{50} i.p. in mice: 1500 mg kg^{-1}), have been disclosed as capable of revealing strong antinociception in dose ranges of 0.00625–0.1 LD_{50} (12.5–200 mg) and 0.0125–0.1 LD_{50} (18.75–150 mg), respectively, in the acetic acid-induced writhing test of mice [8, 9]. The most potent structure with a *meta*-chloro group attached to the phenyl ring (**6**) and the parent compound, which is deprived of any substituent at the phenyl ring (**1**), have previously been suggested as possible opioid analgesics because their in vivo analgesic effects were reversed by a commonly acceptable dose of naloxone (an opioid antagonist) [8, 9].

In previous studies, for all these bioactive substances (**1–6**), the statistically significant relationships were found between their chromatographic partitioning parameters (determined on the cholesterol column) and descriptors of pharmacokinetic bioactivity such as the ability of penetration of the blood–brain barrier, the human serum albumin binding properties, the human intestinal absorption and effective permeability) [10].

The thermal behaviour of this class of compounds was not investigated in the past. All these compounds (**1–6**), having sharp melting points [8], were employed in the present study as a set of the targeted analytes because of their possible use as candidates for pharmaceutical application. They seem to be of significance with regard to their anticipated antinociceptive [8, 9] and antiproliferative [11] fields of relevance. We hope that from this set of bioactive and bioavailable compounds, particularly the two strongly analgesic active and relatively low toxic lead structures (**5** and **6**) will be applied in the future in medicine.

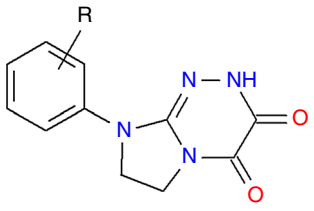

Scheme 1 Structures of the investigated compounds. **1**. R = H, **2**. R = 2–CH_3, **3**. R = 4–CH_3, **4**. R = 2–CH_3O, **5**. R = 4–CH_3O, **6**. R = 3–Cl

Experimental

Synthesis and short description of compounds 1–6

The synthesis of the compounds investigated was achieved by reacting equimolar ratios of 1-arylimidazolidin-2-one hydrazones with diethyl oxalate in boiling *n*-butanolic medium, as previously patented and described [8, 9]. Full structural characterization of these derivatives has been previously published (elemental analyses (C, H, Cl, N), ^{1}H NMR, ^{13}C NMR, EI–MS spectral data, including the solved X-ray crystal structure of compound **2**, having as R an *ortho*-methyl group joined to the phenyl ring) [8, 9, 11]. Biological activities in vivo and in vitro, RP-HPLC-derived lipophilicity indices and computed log *P* values, the correlation between estimated experimentally log ($1/LD_{50}$) values and determined log P_{HPLC} indices, and the remarkable relationships between lipophilicity indices and in silico biological descriptors for 8-ATHITDs have previously been extensively studied and described [8–12]. Furthermore, the electron-ionization mass spectra, the specific fragmentation pathways of the compounds under study and the problem of tautomerism in the gas phase were the subject of an earlier paper [13].

Methods and physical measurements

Thermal stability and decomposition of the analysed compounds were determined by Setaram Setsys 16/18 derivatograph, recording TG, DTG and DSC curves. The samples (4.84–5.99 mg) were heated in ceramic crucible between 30 and 800 °C [850 °C for (**1**)] in flowing air atmosphere ($v = 0.75$ dm^3 h^{-1}) with a heating rate of 10 °C min^{-1}. The temperature and heat flow of the instrument were calibrated by the melting point and enthalpy of indium standard. TG–infrared spectrometry (TG–FTIR) of the title compounds was performed using the TG Q5000 analyser (TA Instruments, New Castle, Delaware, USA)

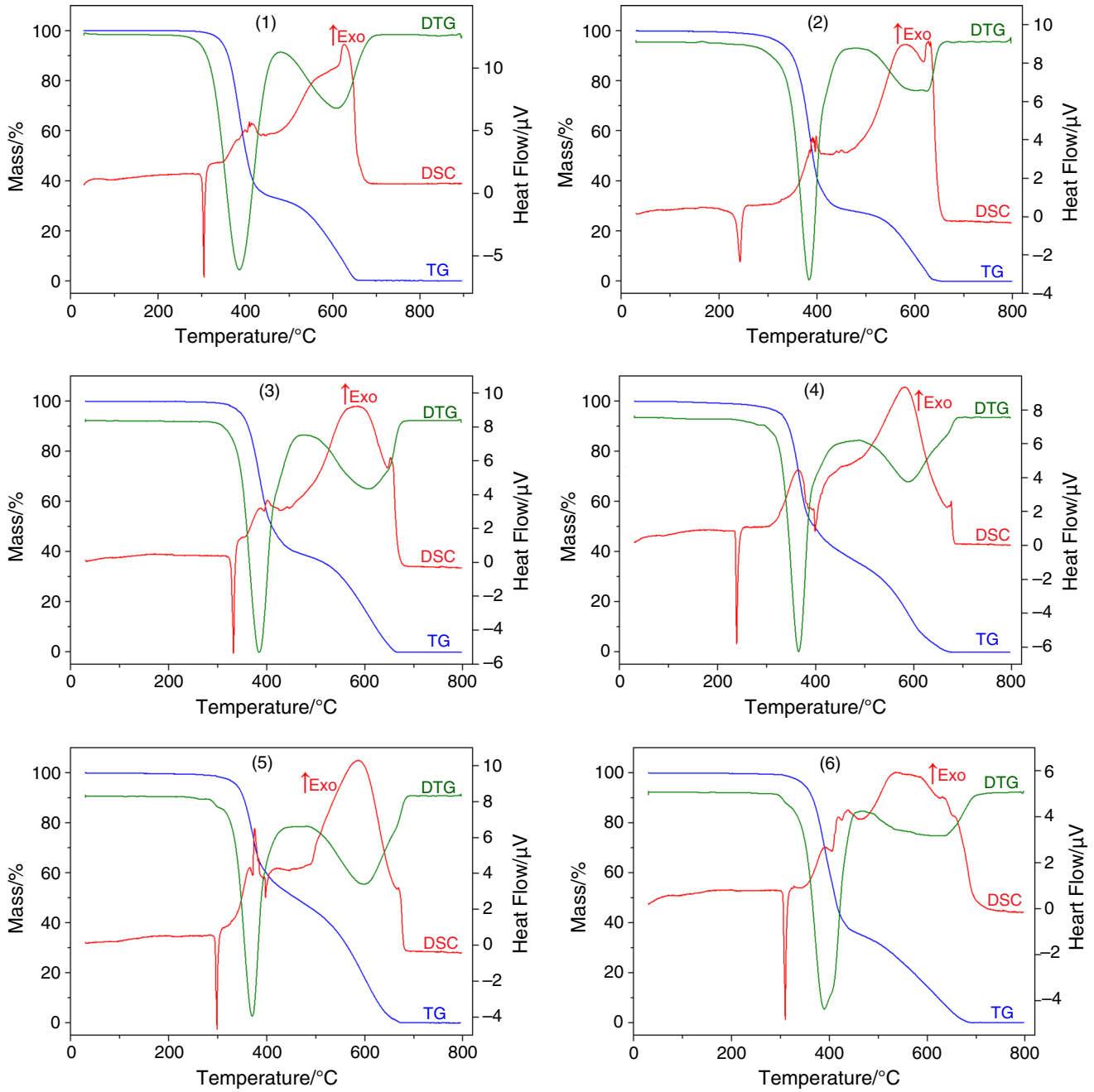

Fig. 1 TG, DTG and DSC curves for the compounds **1**–**6** in air

interfaced to the Nicolet 6700 FTIR spectrophotometer (Thermo Scientific). About 13.60–22.27 mg of compounds were put in an open platinum crucible and heated from an ambient temperature (~23–25 °C) to 1000 °C. The analyses were carried out at a heating rate of 20 °C min^{-1} under nitrogen atmosphere at a flow rate of 25 mL min^{-1}. In order to reduce the possibility of gases condensing along the transfer line, the temperature in the gas cell and transfer line was set to 250 and 240 °C, respectively. The FTIR spectra were recorded in the spectral range of 600–4000 cm^{-1} with a resolution of 4 cm^{-1} and six scans per spectrum.

Results and discussion

Thermal analyses of the investigated compounds were carried out by the TG–DSC (air) and TG–FTIR (nitrogen) techniques. TG–DSC curves providing information about thermal properties of the compounds are shown in Fig. 1.

Table 1 Results of the melting process

Compound	T_{onset}/°C	T_{peak}/°C	ΔH_m/J g^{-1}	ΔH_m/kJ mol^{-1}
1	301	305	113.49	26.13
2	233	243	104.98	25.64
3	327	332	115.77	28.28
4	236	239	91.07	23.70
5	294	298	79.93	20.80
6	305	309	85.70	22.68

The TG–DSC curves show that the studied compounds are thermally stable under air stream up to ~200 °C. All the investigated compounds show their first DSC peak (attributed to melting accompanied by the negligible mass loss) in the temperature range 236–327 °C. These endothermic peaks are connected with melting process which is characteristic for studied compounds [9]. The melting point onset temperature (T_{onset}), peak temperature (T_{peak}) corresponding to each peak and the enthalpy of fusion taken from DSC curves for all compounds are summarized in Table 1. This DSC peak is sharp for all studied compounds (except compound **2**) which indicating that they are crystalline, pure substances (see Fig. 1). In case of sample **2**, the melting peak on DSC curve is distorted in shape and the melting process is only characterized by the temperature of its peak maximum. The previous studies, X-ray single crystal, HPLC and TLC analyses [10–12], indicate that compound **2** is also the crystalline, pure substance, so the shape of the peak is not due to its contamination.

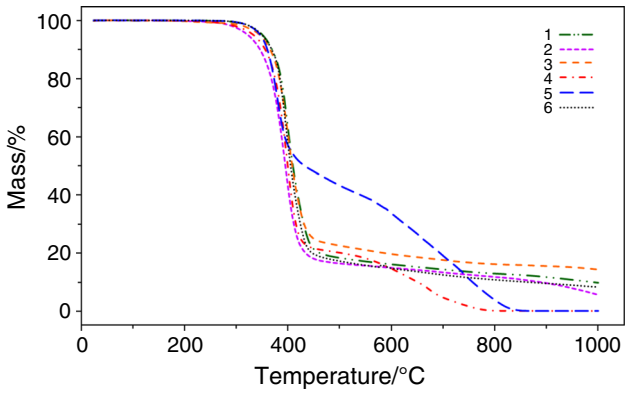

Fig. 2 TG curves for studied compounds **1**–**6** in nitrogen

Probably, the shape of the peak is affected by the molecular structure of **2**. According to data obtained from X-ray single crystal analysis [11], the presence of strong intermolecular N–H···O hydrogen bonds involving one nitrogen of the triazine ring and carbonyl atom leads to the formation of dimers. Further, the structure is stabilized by π–π interactions which extend structure into polymeric supramolecular assembly. The melting point of **2** determined from DSC curve (243 °C) is in a good agreement with the previously reported value (241–243 °C, determined on a Boetius apparatus [9]). According to the literature, the melting points do generally increase with increasing molecular mass except where the increase in molar mass is due to a substitution that makes the molecule less symmetrical [14–17]. This rule can be observed in the case of

Table 2 TG and DSC data of compounds **1**–**6**

Compound	Atm	Step 1				Step 2			
		T_{onset}/°C	T_{peak}/°C	T_{final}/°C	W/%	T_{onset}/°C	T_{peak}/°C	T_{final}/°C	W/%
1	Air	305	386	465	66.65	472	608	668	33.06
	N_2	284	395	503	81.74	–	–	–	–
2	Air	269	384	461	71.58	471	602 624	657	28.11
	N_2	245	395	471	82.87	–	–	–	–
3	Air	327	384	467	60.71	469	607	674	39.09
	N_2	261	401	481	76.74	–	–	–	–
4	Air	261	365	452	60.38	453	588	687	39.58
	N_2	237	398	461	78.77	503	671	804	21.06
5	Air	295	370	446	48.72	451	599	679	51.15
	N_2	282	379	457	52.68	517	695	854	47.16
6	Air	305	389	454	63.92	455	608	699	36.01
	N_2	286	397	485	82.21	–	–	–	–

Atm, atmosphere of analysis; T_{onset}, onset degradation temperature; T_{final}, final degradation temperature; T_{peak}, DTG peak temperature (maximum change of mass); W, mass loss

Table 3 Gaseous products evolved during thermal decomposition of the compounds **1**–**6** in a nitrogen atmosphere

Gaseous species	*T*/°C					
	1	**2**	**3**	**4**	**5**	**6**
H_2O	305–1000	250–1000	270–1000	245–810	300–860	305–1000
CO_2	305–1000	250–1000	270–1000	245–810	300–860	305–1000
CO	350–440	265–465	280–470	265–550	330–590	340–490
	590–1000	585–1000	610–1000			600–1000
NH_3	380–1000	300–1000	385–1000	305–630	345–645	385–1000
HCN	380–460	305–485	395–505	340–450	350–445	395–520
	540–590	525–595	550–585	522–540	565–575	530–800
HNCO/RNCO	380–590	305–595	395–585	340–540	350–575	395–665
Aniline or its derivative	395–590	390–485	395–505	340–550	355–580	410–505
		530–565	655–660			
Carbonyl compounds	395–590	530–565	655–660	340–545	360–580	–
CH_4	–	–	–	420–550	425–585	–

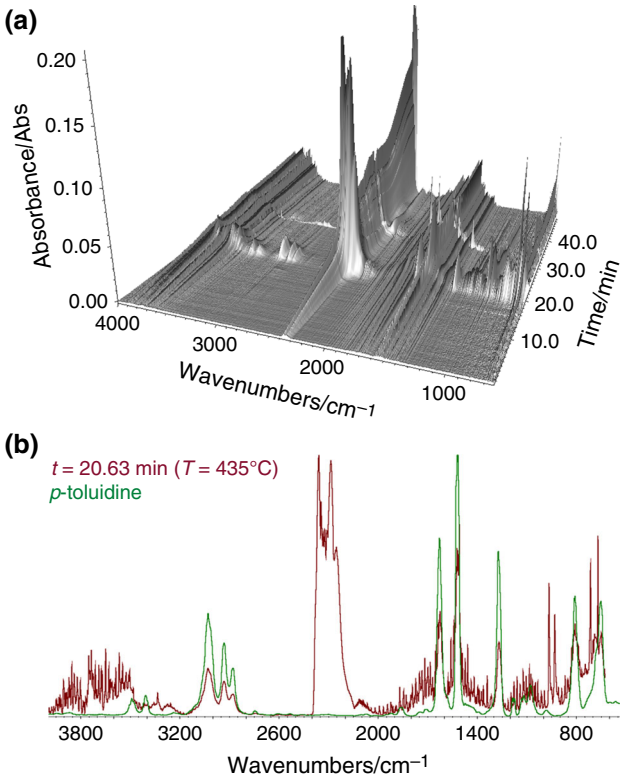

Fig. 3 **a** FTIR spectra of gaseous products evolved during the decomposition of **3**; **b** FTIR spectra of *p*-toluidine in gas state and gaseous products of **3** decomposition at 435 °C

studied compounds if we consider them as derivatives of benzene. Among disubstituted benzene derivatives, the melting point of the more symmetrical *para* compound is higher than those of the *ortho* and *meta* isomers. Between *ortho* and *meta* isomers, the former is more symmetrical [16, 17]. In our studies, the *ortho* derivatives (compounds **2** and **4**) reveal lower melting points than those *para* analogues (**3** and **5**). The high melting point of *meta*-disubstituted benzene derivative (compound **6**) can be connected with the presence of electronegative Cl atom in the structure which can be engaged in strong polar interactions like H-bonding and the symmetry as a factor becomes less important [16, 17].

The decompositions of the compounds in air are a two-step process that is noted on the TG curves (see Fig. 1). The first major mass loss steps are observed in the temperature ranges of 261–327 °C and occurred together with the melting process for all compounds with exception of compounds **2** and **4**. The decomposition temperature of **2** and **4** is found to be about 25 °C higher than the melting point. For this reason, an order of melting points and thermal stabilities of compounds calculated from TG and DSC curves follows in the similar order, i.e. $\mathbf{3} > \mathbf{6} \approx \mathbf{1} > \mathbf{5} > \mathbf{2} \approx \mathbf{4}$. This stage is connected with the partial destruction and combustion of the samples. Within this first step of compounds decomposition, more than fifty per cent of mass loss is observed (Table 2) for all investigated compounds (with exception of **5**) and intermediate, unstable products are formed. The second stage above 451–472 °C corresponds to the complete destruction and combustion of the remaining parts of the compounds. The samples are fully decomposed at a temperature of approximately 600 °C (the compound **4** burns completely in a bit lower temperature 588 °C).

Thermal behaviour of **1**–**6** was also studied in nitrogen atmosphere (see Fig. 2). In case of compounds **4** and **5**, on TG curves two changes of mass are observed and samples are almost completely burnt (the residues left after a decomposition are less than 0.2 %). The first step of decomposition of these compounds starts at 237 °C for **4** and

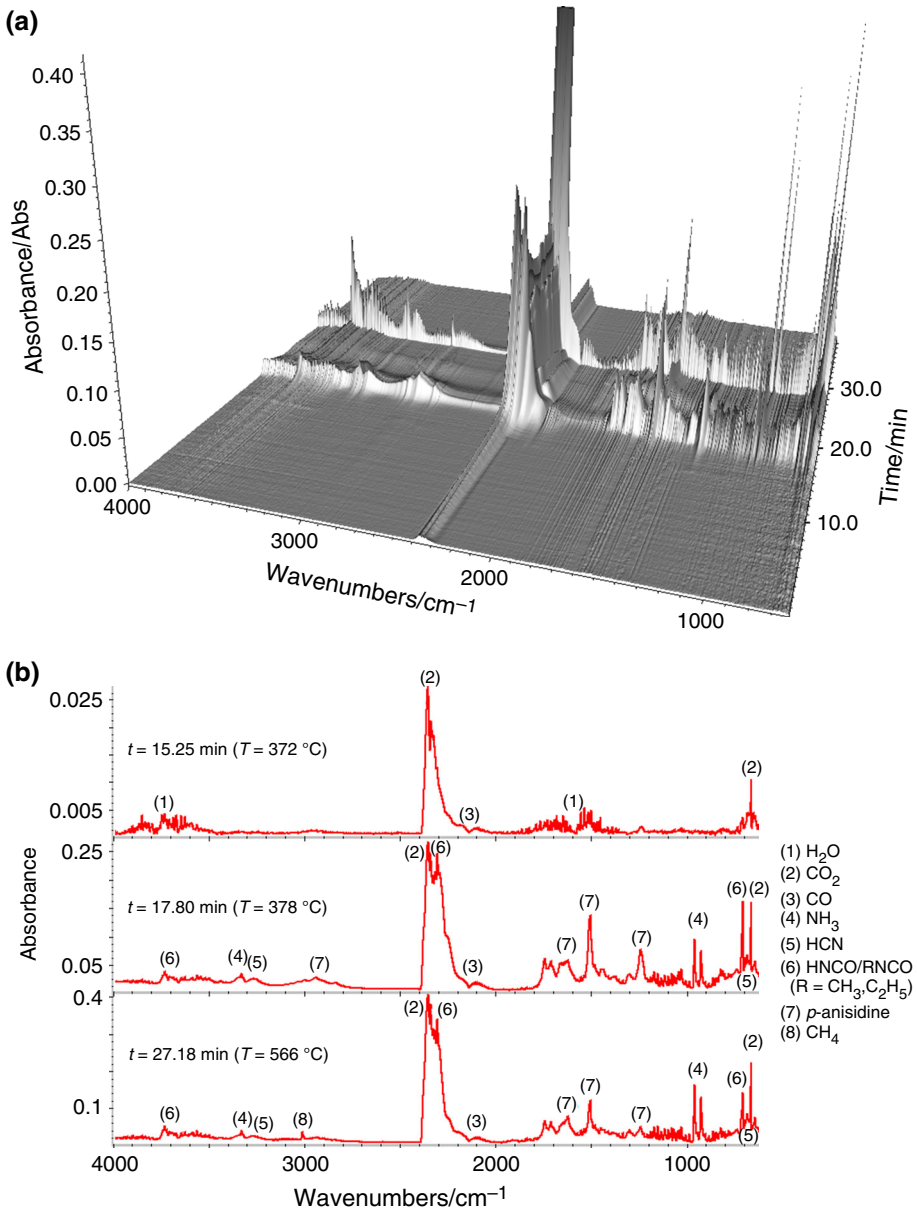

Fig. 4 **a** FTIR spectra of gaseous products evolved during the decomposition of **5**; **b** FTIR spectra of gaseous products of **5** decomposition at 372, 378 and 566 °C

282 °C for **5.** The intermediate products are formed at temperature 461 and 457 °C with the mass loss over 78 and 52 % for compounds **4** and **5**, respectively. The next step of decomposition starts at above 500 °C and corresponds to a complete destruction and degradation of the remaining parts of the compounds. For the remaining compounds, one major mass loss steps on TG curves are noted and decompositions are not completed. Compounds **1**–**3** and **6** are thermally stable up to 245–286 °C and then decompose with the initial mass loss more than 75 % (see Table 2). During this step, the partial destructions and combustions of compounds are observed. The further heating causes slow decomposition and thermal degradation of the rest of the compounds, but it is not clearly marked on the DTG curves of **1**–**3** and **6**. The differences in mass loses after the first decomposition step of **1**–**3** and **6**, which are marked with a peak on the DTG curves, and the final temperature (1000 °C) are 8.5–11.5 %. Together with TG analysis in nitrogen, the FTIR spectra of the gaseous products were recorded (Table 3). The FTIR spectra of gaseous products evolved during the decomposition of compounds **3** and **5** are presented on Figs. 3 and 4, respectively. At the beginning of the decomposition process of investigated compounds, the main gaseous products emitted at around 245–305 °C are identified as H_2O, CO_2 and CO (see Table 3; Figs. 3, 4). Carbon dioxide refers to double band at 2240–2400 cm^{-1} derived from stretching vibration, ν(C–O). In additional, a band at 669 cm^{-1} was observed due to the deformation vibration of CO_2 molecules. The double peaks corresponding to CO are recorded in the

range at 2050–2275 cm^{-1}. The characteristic bands of water molecules, stretching and deformation vibrations, are observed in the range 3450–4000 cm^{-1} and 1300–1950 cm^{-1}, respectively [18–22]. Further heating causes an increase in the emission of these gaseous species as well as a new products are observed. FTIR spectra of **1–6** show band characteristic of NH_3 which appears around 14–18 min (300–385 °C). The emission of ammonia is confirmed by the appearance of absorption bands at 3334, 966 and 931 cm^{-1} [18, 22–25]. This gas together with other small molecules (H_2O and CO_2) is evolved during the whole further analysis of **1–3** and **6**. Almost in the same temperature as ammonia in mixtures of emitted gases, hydrogen cyanide (HCN) and isocyanic acid (HNCO, probably with its derivatives, i.e. methyl and ethyl isocyanates) are appeared. The most characteristic, qualitative bands for HNCO and its derivatives are observed at 2200–2300 cm^{-1} (see Fig. 4b) [18, 22, 23, 26]. On the FTIR spectra of evolved volatile pyrolysis products, the vibrations assigned to HCN occur at 3336, 3273, 714 cm^{-1} [23, 26]. In gaseous products of thermal decomposition, the bands characteristic of aniline or its derivatives such as *o*-toluidine, *p*-toluidine, *o*-anisidine, *p*-anisidine or *m*-chloroaniline were also recorded. The presence of these specific types of compounds (i.e. aniline or its derivative) in gaseous products evolved during the thermal decomposition depends on the substitution of the benzene ring (see Figs. 3b, 4b). Additional absorption bands at ~1750 and ~1716 cm^{-1} are observed, but we could not identify the gases corresponding to those peaks. This region is characteristic for carbonyl compounds [27]. In case of compounds **4** and **5**, on the end of first step of decomposition around 20 min (~420 °C) several bands characteristic of CH_4 were observed (in the range 3175–2900 cm^{-1} with a characteristic maximum at 3016 cm^{-1} [7, 18, 27]). Probably, the methane is released at a lower temperature, but the vibrations were covered by the bands of anisidine. At the beginning of the second step of **4** and **5** decomposition process, the following molecules were identified in a mixture of gaseous products: CO_2, CO, CH_4, NH_3, HCN, HNCO, anisidine and carbonyl compounds. Most of these gases disappear at ~550 °C (**4**) and ~585 °C (**5**), and on the FTIR spectra of evolved volatile pyrolysis products, mainly bands of water, carbon dioxide and trace amounts of NH_3 were recorded (Table 3).

Conclusions

Thermal analysis of the six analgesic active derivatives of 8-ATHITD was performed. Thermal stability and the melting point of compounds have been studied by TG–DSC analysis in air atmosphere. The investigated compounds are stable at room temperature which is important for medical application as well as during the storage and processing by pharmaceutical industry. DSC melting peaks of compounds (with exception **2**) are sharp, indicating that they are crystalline, pure substances. The purity of compound **2** was confirmed by chromatographic analysis and X-ray single structure determination. The fact that compounds **1–6** have been synthesized in the crystalline form is their advantage because amorphous compounds are less thermodynamically stable and have a tendency to transform to a known or potentially unknown crystalline phase. In air atmosphere, decomposition process of **1–6** occurs in two stages. The scheme of thermal behaviour in air of the investigated compounds is as follows:

compound $\overset{\sim 236-327^{\circ}C}{\longrightarrow}$ melting process $\overset{\sim 261-327^{\circ}C}{\longrightarrow}$ decomposition (intermediate formation) $\overset{\sim 451-472^{\circ}C}{\longrightarrow}$ complete decomposition and combustion.

On the basis of TG–DSC analysis, it can be concluded that the substitution of a hydrogen by methoxy group on the benzene ring in the *ortho* or *para* positions leads to lower thermal stability of the studied 8-ATHITDs. Moreover, the *para* isomers (**3** and **5**) are found to be more thermal stable than their *ortho* analogues (**2** and **4**) as a consequence of a higher symmetry of the compounds. The performed TG–FTIR analysis showed that there are no residual solvents in structure of studied compounds and they are not hygroscopic. What is more, this technique confirmed the formation of various compounds during pyrolysis of **1–6**. The following gases CO_2, CO, NH_3, HCN, HNCO (and its derivatives), aniline or its derivatives and carbonyl compounds are main volatile decomposition products of pyrolysis.

References

1. Ford JL, Timmins P. Pharmaceutical thermal analysis: techniques and applications. Chichester: Ellis Horwood; 1989.
2. Giron D. Thermal analysis of drugs and drug products. Encyclopedia of pharmaceutical technology. 3rd ed. Pinehurst: Taylor & Francis; 2013. p. 3726–51.
3. Giron D. Applications of thermal analysis and coupled techniques in pharmaceutical industry. J Therm Anal Calorim. 2002;68:335–57.
4. Aneja DK, Kumar M, Prakash O, Arora S. Thermal studies of some biological sctive *bis*[1, 2, 4]triazolophthalazines: non isothermal kinetic study of one of the potent 3,6-*bis*(4-nitrophenyl)*bis*([1, 2, 4]triazolo)[3,4-a:4′,3′-c] phthalazine. Chem Sci Trans. 2013;2:941–9.
5. Brown ME, Gallagher PK. Handbook of thermal analysis and calorimetry: recent advances, techniques and applications. Amsterdam: Elsevier; 2011.
6. Cheng H, Liu Q, Liu J, Sun B, Kang Y, Frost R. TG–MS–FTIR (evolved gas analysis) of kaolinite–urea intercalation complex. J Therm Anal Calorim. 2014;116:195–203.
7. Bassilakis R, Carangelo RM, Wójtowicz MA. TG–FTIR analysis of biomass pyrolysis. Fuel. 2001;80:1765–86.

8. Sztanke K, Fidecka S, Matosiuk D. New 3-hydroxy-4-oxo-8-aryl-7,8-dihydro-6*H*-imidazo[2,1-*c*][1,2,4] triazine and method for their manufacture. PL Patent 196752; Poland; 2003.
9. Sztanke K, Fidecka S, Kędzierska E, Karczmarzyk Z, Pihlaja K, Matosiuk D. Antinociceptive activity of new imidazolidine carbonyl derivatives. Part 4. Synthesis and pharmacological activity of 8-aryl-3,4-dioxo-2*H*,8*H*-6,7-dihydroimidazo[2,1-c][1,2,4]triazines. Eur J Med Chem. 2005;40:127–34.
10. Janicka M, Sztanke M, Sztanke K. Reversed-phase liquid chromatography with octadecylsilyl, immobilized artificial membrane and cholesterol columns in correlation studies with in silico biological descriptors of newly synthesized antiproliferative and analgesic active compounds. J Chromatogr A. 2013;1318:92–101.
11. Sztanke K, Pasternak K, Rzymowska J, Sztanke M, Kandefer-Szerszeń M, Dybala I, et al. Identification of antitumour activity of novel derivatives of 8-aryl-2,6,7,8-tetrahydroimidazo[2,1-*c*][1,2,4]triazine-3,4-dione and 8-aryl-4-imino-2,3,7,8-tetrahydroimidazo[2,1-*c*][1,2,4]triazin-3(6*H*)-one. Bioorg Med Chem. 2007;15:2837–49.
12. Sztanke K, Markowski W, Swieboda R, Polak B. Lipophilicity of novel antitumour and analgesic active 8-aryl-2,6,7,8-tetrahydroimidazo[2,1-*c*][1,2,4]triazine-3,4-dione derivatives determined by reversed-phase HPLC and computational methods. Eur J Med Chem. 2010;45:2644–9.
13. Martiskainen O, Sztanke K, Matosiuk D, Pihlaja K. Electron ionization mass spectra of 8-aryl-3,4-dioxo-2*H*,8*H*-6,7-dihydroimidazo[2,1-*c*][1,2,4]triazines. Do they exhibit tautomerism in the gas phase? Rapid Commun Mass Spectrom. 2006;20:2548–52.
14. Arora S, Aneja DK, Kumar M, Sharma C, Prakash O. Thermal studies of some biological active oxadiazoles Non-isothermal kinetic study of potent antibacterial 2-(4-chlorophenyl)-5-(thiophen-2-yl)-1,3,4-oxadiazole. J Therm Anal Calorim. 2013;111:17–25.
15. Smith MB. Organic chemistry: an acid–base approach. Boca Raton: CRC Press; 2011.
16. Brown RJC, Brown RFC. Melting point and molecular symmetry. J Chem Educ. 2000;77:724–31.
17. Prahlada Rao S, Sunkada S. Making sense of boiling points and melting points. Resonance. 2007;12:43–57.
18. Bartyzel A. Synthesis, crystal structure and characterization of manganese(III) complex containing a tetradentate Schiff base. J Coord Chem. 2013;66:4292–303.
19. Ostasz A, Łyszczek R, Mazur L, Sienkiewicz-Gromiuk J, Rusinek I, Rzaczynska Z. Some properties of Nd and Er complexes with 1,2,3,4,5,6-benzenehexacarboxylic (mellitic) acid. J Anal Appl Pyrolysis. 2013;99:203–10.
20. Łyszczek R. Hydrothermal synthesis, thermal and luminescent investigations of lanthanide(III) coordination polymers based on the 4,4'-oxybis(benzoate) ligand. J Therm Anal Calorim. 2012;108:1101–10.
21. Yan J, Jiang X, Han X, Liu J. A TG-FTIR investigation to the catalytic effect of mineral matrix in oil shale on the pyrolysis and combustion of kerogen. Fuel. 2013;104:307–17.
22. Girods P, Dufour A, Rogaurne Y, Rogaurne C, Zoulalian A. Pyrolysis of wood waste containing urea-formaldehyde and melamine-formaldehyde resins. J Anal Appl Pyrolysis. 2008;81:113–20.
23. Jiang X, Li C, Chi Y, Yan J. TG–FTIR study on urea-formaldehyde resin residue during pyrolysis and combustion. J Hazard Mater. 2010;173:205–10.
24. Rzączyńska Z, Bartyzel A, Głowiak T. Crystal structure, thermal analysis and spectroscopic study of sodium 3,4-diaminobenzoate. J Coord Chem. 2003;56:77–83.
25. Łyszczek R, Mazur L. Polynuclear complexes constructed by lanthanides and pyridine-3,5-dicarboxylate ligand: structures, thermal and luminescent properties. Polyhedron. 2012;41:7–19.
26. Hao J, Guo J, Ding L, Xie F, Xia Q, Xie J. TG–FTIR, Py-two-dimensional GC–MS with heart-cutting and LC–MS/MS to reveal hydrocyanic acid formation mechanisms during glycine pyrolysis. J Therm Anal Calorim. 2014;115:667–73.
27. Caires FJ, Gomes DJC, Gigante AC, Ionashiro M. Thermal investigation and infrared evolved gas analysis of solid trivalent lanthanide and yttrium α-hydroxyisobutyrates in N_2 and CO_2 atmospheres. J Anal Appl Pyrolysis. 2014;107:313–22.